GASP-2 overexpressing mice exhibit a hypermuscular phenotype with contrasting molecular effects compared to GASP-1 transgenics

Alexis Parenté, Axel Boukredine, Fabienne Baraige, Nathalie Duprat, Victor Gondran-Tellier, Laetitia Magnol, Véronique V. Blanquet

Received: 15 May 2019 | Revised: 27 October 2019 | Accepted: 31 December 2019

DOI: 10.1096/fj.201901220R

RESEARCH ARTICLE

THE FASEB JOURNAL

GASP-2 overexpressing mice exhibit a hypermuscular phenotype with contrasting molecular effects compared to GASP-1 transgenics

Alexis Parenté | Axel Boukredine | Fabienne Baraige | Nathalie Duprat | Victor Gondran-Tellier | Laetitia Magnol | Véronique Blanquet

INRA, PEIRENE EA7500, USC1061 GAMAA, Université de Limoges, Limoges, France

Correspondance
Véronique Blanquet, INRA, PEIRENE EA7500, USC1061 GAMAA, Université de Limoges, 123, av. A. Thomas, F-87060 Limoges, France.
Email: veronique.blanquet@unilim.fr

Funding information
European Union; Limousin Regional Council; French National Institute for Agricultural Research

Abstract

Muscle atrophy is associated with many diseases including genetic disorders, sarcopenia, or cachexia syndromes. Myostatin (*Mstn*), a transforming growth factor-beta (TGF-β) member, plays a key role in skeletal muscle homeostasis as a powerful negative regulator. Over the last decade, about 15 clinical trials aimed at inhibiting the *Mstn* pathway, failed to produce conclusive results. In this context, we investigated whether growth and differentiation factor-associated serum protein-1 (GASP-1) or GASP-2, two natural inhibitors of *Mstn*, might represent a potential therapeutic. As we previously reported, mice overexpressing *Gasp-1* (*Tg(Gasp-1)*) present an increase of muscle mass but develop metabolic disorders with aging. Here, we showed that overexpression of *Gasp-2* increases the muscular mass without metabolic defects. We also found that *Tg(Gasp-2)* mice displayed, like $Mstn^{-/-}$ mice, a switch from slow- to fast-twitch myofibers whereas *Tg(Gasp-1)* mice exhibit a reverse switch. Our studies supported the fact that GASP-2 has less affinity than GASP-1 for *Mstn*, leading to a constitutive *Mstn* upregulation only in *Tg(Gasp-1)* mice, responsible for the observed phenotypic differences. Altogether, our findings highlighted a gene expression regulatory network of TGF-β members and their inhibitors in muscle.

KEYWORDS

muscle, myostatin, GASP-1, GASP-2, hypertrophy, hyperplasia

1 | INTRODUCTION

Many diseases (neuromuscular or chronic inflammatory diseases, cancer...) are associated with skeletal muscle atrophy. Muscle wasting occurs also as a natural process of aging and can lead to sarcopenia, a generalized loss of muscle mass and function. These muscle tissue defects are highly disabling for patients, especially since there is a lack of adequate

Abbreviations: β2m, beta-2-microglobulin; Ccr5, C-C chemokine receptor type 5; CMV, cytomegalovirus; Gapdh, glycéraldéhyde-3-phosphate deshydrogenase; Gasp, growth and differentiation factor-associated serum protein; GDF, growth and differentiation factor; Mstn, myostatin; Mrf-4, myogenic regulatory factor4; MyHC, myosin heavy chain; Myog, myogenin; Pax7, paired box 7; Smad2/3, Sma mothers against decapentaplegic homolog; Tg, transgenic; TGF-β, transforming growth factor-beta.

Laetitia Magnol and Véronique Blanquet are considered co-last authors and contributed equally to this work.

treatments.[1] Improving our understanding of the mechanisms responsible for skeletal muscle atrophy in patients is important in order to develop therapies to prevent these clinical conditions.

Skeletal muscle is composed of heterogeneous muscle fibers bundled together and which differ in their metabolism and contractile properties.[2,3] This type of organization confers to skeletal muscle remarkable levels of plasticity in the face of changes to the external environment. During embryonic development, the number and the size of myofibers increase (hyperplasic and hypertrophic growth) until birth.[4] Postnatal muscle growth is then only achieved by myofibers hypertrophy and can be divided into two distinct steps. Between birth and weaning in mouse, hypertrophy is supported by a rapid increase of the nuclei number within myofibers via the activation and fusion of satellite cells.[5] From 3 weeks old to adulthood, muscle mass regulation is dependent of a balance between protein synthesis and degradation. This protein turnover is induced in response to various stimuli such as exercise, inactivity, or environmental factors (hypoxia, heat, nutrient availability, and growth factors).[6] During the past two decades, much progress has been made in unraveling the molecular mechanisms underlying either adult muscular hypertrophy or atrophy.[6,7]

Myostatin (*Mstn)*, a member of the transforming growth factor-beta (TGF-β) superfamily, is an important negative regulator of skeletal muscle growth, homeostasis and repair.[8,9] Myostatin knockout ($Mstn^{-/-}$) mice exhibit at 3 months an increase in muscle mass due to both hyperplasia and hypertrophy of myofibers. *Mstn* -null mice have reduced body fat and increased tolerance to glucose, protecting them from age-related obesity.[10,11] Targeting the *Mstn* signaling pathway may offer promising therapeutic strategies for the treatment of muscle wasting disorders.[12] Although several clinical trials by inhibiting *Mstn* are conducted, the first results are controversial except in a gene therapy trial based on the inhibition of *Mstn* by follistatin, one of its natural inhibitors.[13,14] In this context, we investigated whether the paralogs growth and differentiation factor-associated serum protein-1 (GASP-1) and GASP-2, two other natural *Mstn* inhibitors, might represent a potential therapeutic.

Growth and differentiation factor-associated serum protein-1 and GASP-2 are two closely related multi-domain glycoproteins, playing a role of chaperones for some TGF-β members and are able to inhibit in vitro *Mstn* and growth and differentiation factor-11 (GDF-11), a *Mstn* -homologous protein.[15,16] GASP-1 or GASP-2 overexpression promotes proliferation and differentiation of C2C12 myoblast cells by inhibiting the *Mstn* pathway.[17,18] As we have shown, transgenic *Tg(Gasp-1)* mice overexpressing *Gasp-1* present a hypermuscular phenotype associated with hypertrophy without hyperplasia and exhibit no decrease in fat mass at 3 months.[19] Surprisingly, we found that these mice gained weight with age and developed muscle/hepatic insulin resistance.[20] Molecular analyses revealed an upregulation of *Mstn* from the embryonic stage and throughout life, responsible for the absence of hyperplasia and metabolic defects in *Tg(Gasp-1)* mice.[20,21] Thus, GASP-1 does not constitute a good drug candidate with a high therapeutic potential.

Here, we investigated the effects of the overexpression of *Gasp-2* by generating and characterizing the *Tg(Gasp-2)* mice. Phenotypic analyses revealed that the *Tg(Gasp-2)* exhibit an increase of muscle mass due to a myofiber hypertrophy without hyperplasia as previously shown in *Tg(Gasp-1)* mice. Interestingly, the *Tg(Gasp-2)* mice do not develop metabolic defects. At the molecular level, we showed that the *Tg(Gasp*-2) mice exhibit an upregulation of GDF-11 and a downregulation of several *Mstn* inhibitors, leading to the absence of hyperplasia. Our findings highlighted a functional duality between GASP-1 and GASP-2 as well as a gene expression regulatory network of TGF-β members and their inhibitors in muscle at the embryonic stage.

2 | METHODS

2.1 | Animals

Myostatin deficient mice *($Mstn^{-/-}$)* and *Gasp-1* overexpressing mice (*Tg(Gasp-1)*) have been described previously.[19,22] The generated transgenic lines *Tg(Gasp-2)* overexpressing *Gasp-2*, *$Mstn^{-/-}$, Tg(Gasp-1),* and control animals are on FVB/N background. All mice were bred and housed in the animal facility of Limoges University under controlled conditions (20°C, 12 hours light/12 hours dark cycle) with free access to standard mouse chow and tap water. Experimental procedures were carried out in accordance with European legislation on animal experimentation (Directive 2010/63/UE) and approved by the ethical committee n°033 (APAFIS #1903-2015091612088147 v2).

Phenotypic and molecular analyses were performed on 3-weeks-old, 3-month-old, and 16-month-old mice, independently of animal sex.

2.2 | Generation of transgenic lines overexpressing *Gasp-2*

The 1656 bp coding sequence of the murine *Gasp-2* gene was amplified by primers 5′-ATGCCTGCCCCACAGCCATTC-3′ and 5′-GTCTTGGAAGCGGTTGAGCAGTTC-3′ (transcript sequence ENSEMBL ENSMUSG-00000071192) and was introduced into the expression vector pcDNA3.1/V5-His TOPO (Invitrogen) where *Gasp-2* cDNA is under the cytomegalovirus (CMV) promoter/enhancer. A purified Sal1-NsiI fragment was microinjected into the male pronucleus

of one-cell fertilized FVB/N embryos. Two independent homozygous lines overexpressing *Gasp-2*, named *Tg(Gasp-2.2),* and *Tg(Gasp-2.9)*, were obtained from two different founders and were characterized.

2.3 | Copy number genotyping

Copy number genotyping was done using SYBR Green–based Real-Time PCR from *Tg(Gasp-2)* genomic DNA (QuantStudio 3 system, ThermoFisher Scientific). To determine the average inserted *Gasp-2* transgene copy number, we used C-C chemokine receptor type 5 (*Ccr5)* as endogenous reference gene to normalize the amount of chromosomal DNA (number of transgene copy number by cell = 2 ΔCt X2 – 2). PCR assays were carried out as previously described in Monestier et al[19] using the following primers: *Gasp-2*-Fwd (5′ATGCGCCCTGACCAAATGTA 3′) and *Gasp-2*-Rev (5′-CTGTCCTGAGTAGTTGCCCG-3′) primers targeting *Gasp-2* exon 2; *Ccr5*-Fwd (5′-GCACAAAGAGACTTGAGGCA-3′) and *Ccr5*-Rev (5′-GTCATCTCTAGGCCACAGCA-3′) primers targeting *Ccr5* exon 2. Data were analyzed by the QuantStudio Design & Analysis software.[19]

2.4 | RNA extraction, retrotranscription and gene expression analysis

Total RNA from tissues, cells, or embryos were isolated using RNeasy midi kit (Qiagen). Synthesis of cDNA was performed with the High Capacity cDNA Archive kit (Applied Biosystems) to convert 2 μg of total RNA into single-stranded cDNA. Taqman copy number assays were done with Gene Expression Master Mix (Applied Biosystems, ThermoFisher Scientific, Waltham, MA, USA), according to the manufacturer's instructions. Twenty nanograms of cDNA were run in triplicate on QuantStudio 3 real-time PCR system (Applied Biosystem) with Taqman primers and probe sets: *18S* (Hs99999901_s1), glycéraldéhyde-3-phosphate deshydrogenase *(Gapdh)* (Mm99999915_g1), beta-2-microglobulin *(β2m)* (Mm00437762_m1), *Gasp-1* (Mm00725281_m1), *Gasp-2* (Mm01308311_m1), *Mstn* (Mm03024050_m1), Myogenic regulatory factor4 (*Mrf-4)* (Mm00435126_m1), and *Myog* (Mm00446194_m1). Relative mRNA expression values were calculated by the ΔΔCt method with normalization of each sample to the average change in cycle threshold value of the controls.

TaqMan low-density array (TLDA, Applied Biosystems) assays were performed based on the same above conditions, except that 200 ng cDNA were used per TLDA card. TLDA cards present 43 selected genes involved in TGF-β signaling pathway as previously described.[21]

2.5 | Enzyme-linked immunosorbent assay (ELISA) of GASP-2

Growth and differentiation factor-associated serum protein-2concentration from mouse plasma was determined in a sandwich ELISA according to the manufacturer's instructions (GASP-2/WFIKKN DuoSet ELISA, R&D Systems). All measurements were performed in triplicate and data for the standard curve were fitted to a logistic plot with the MARS Data Analysis Software (BMG Labtech) to determine the levels of GASP-2.

2.6 | Protein extraction and immunoblotting

Total cell protein extracts were prepared from frozen tissues or cell pellets, solubilized for 2 hours at 4°C in a RIPA lysis buffer (50 mM Tris, pH 8, 150 mM NaCl, 0.1% SDS, 1% NP-40, 0.5% sodium deoxycholate, and protease inhibitors). Protein lysates were centrifuged at 12 000 g for 20 minutes at 4°C, and protein supernatant concentration was determined at A595 nm using the Bradford assay (Bio-Rad). Equal amounts of proteins (50 μg) were resolved by SDS-PAGE using 10% polyacrylamide gels and then, transferred onto Amersham Protra premium 0.2 μm nitrocellulose (GE Healthcare, Buckinghamshire, UK). Membranes were blocked using 5% nonfat dry milk (w/v) in TBST 0.1% buffer (50 mM Tris-HCl, 150 mM NaCl, pH 7.4, 0.1% Tween-20) for 1 hour at room temperature. Specific primary antibodies were diluted in 2.5% nonfat dry milk and incubated overnight at 4°C: anti-phospho-Sma Mothers Against Decapentaplegic homolog (Smad2/3) (polyclonal Rabbit 1:500, AB3226, R&D Systems), anti-SMAD2/3 (Polyclonal Goat 1:500, AF3797, R&D Systems), anti-V5 (monoclonal mouse 1:1000, MA5-15253, Invitrogen) and anti-mouse GAPDH antibody (Goat polyclonal 1:2000, AF5718, R&D Systems). After three washes with TBST, membranes were incubated with secondary antibodies (anti-goat, anti-rabbit or anti-mouse HRP-conjugated IgG, Dako, Glostrup, Denmark) diluted at 1:1000 in TBST, 2.5% (w/v) nonfat dry milk for 1 hour at room temperature. After three washes in TBST, reactive proteins were visualized with ECL Prime Western blotting system (GE Healthcare, Uppsala, Sweden). For detection and relative quantification of band intensities, we used Amersham Imager 600 device (GE Healthcare).

2.7 | Immunofluorescence staining

Skeletal muscles having a glycolytic, oxidative or mix metabolism (*tibialis anterior*, *gastrocnemius*, *flexor digitorum longus,* and *soleus*) were frozen in liquid nitrogen-cooled isopentane, stored at −80°C and sectioned (10 μm thick). Cryosections were

thawed at room temperature and air-dried. A permeabilization step was required only for paired box 7 (Pax7) staining with cold methanol at −20°C and a treatment for antigen retrieval in 10 mM citrate buffer, pH 6 at 90°C for 2 × 5 min. Then, cryosections were blocked for 1 hour at room temperature in blocking buffer (5% BSA in phosphate buffered saline (PBS)) or (10% goat serum, 1% bovine serum albumin (BSA), and 0.1% Triton X-100 in PBS) for Pax7 staining. Incubation with primary antibodies diluted in BSA 1%/PBS took place overnight at 4°C for Pax7 staining and 1 hour at 37°C for other staining. Primary antibodies used for these analyses were anti-laminin (Rabbit IgG, 1/500, L9393, Sigma-Aldrich), anti-Pax7 (Mouse IgG1, 1/100, MAB1675, R&D System), and different anti-myosin: BA-D5 for Type I (Mouse IgG2b, 1/3, Agro-bio), SC-71 for Type IIa (Mouse IgG1, 1/3, Agro-bio), BF-F3 for type IIb (Mouse IgM, 1/3, Agro-bio), and 6H1 for Type IIx (Mouse IgM, 1/100, DSHB). After washes, slides were incubated for 30 minutes at 37°C with DAPI (1/1000) and secondary antibodies conjugated to a fluorescent dye diluted in BSA 1%/PBS: Alexa-Fluor-350 Goat Anti-Mouse IgG2b, Alexa-Fluor-546 Goat Anti-Mouse IgG1, Alexa-Fluor-488 Goat Anti-Mouse IgM, or Alexa-Fluor-633 Goat Anti-Rabbit IgG (Invitrogen). After washes, the slides are mounted with a coverslip with Mowiol solution and colorless varnish. Scan of the entire muscle area were acquired with an automated Nikon inverted epifluorescence microscope with NIS Element Software. Myofiber area and number were calculated semiautomatically from laminin-stained cryosections using ImageJ software in whole muscle cross sections. Total and $Pax7^+$ myonuclei were automatically counted using ImageJ software. Fiber typing was performed as previously described.[23] Briefly, the fiber type characterization was realized by semiautomatic image analysis Visilog software (FEI), using the double laminin/myosin labelling.

2.8 | Isolation of satellite cell-derived myoblasts and cell culture

Primary myoblasts were obtained from 5-weeks-old male wild-type (WT) or *Tg(Gasp-2.9)* mice. Briefly, murine myoblasts were isolated from hindlimb muscles after enzymatic digestion by pronase (Sigma-Aldrich, P-5147) diluted in Ham's-F10 medium (Gibco) and 1% penicillin/streptomycin, 1 hour at 37°C. The solution was centrifuged for 5 minutes at 800 rpm to remove undigested fragments. The supernatant was filtered on 45 µm cell strainers. The cells are washed three times in Ham's F-10 medium and centrifuged at 1500 rpm for 20 minutes at room temperature. Mouse satellite cells are isolated by depletion of nontarget cells using the Satellite Cell Isolation Kit (Miltenyi Biotec). Cells were plated on Matrigel-coated Petri dishes (BD Biosciences) in Growth Medium (GM): Ham's F10 supplemented with 20% horse serum and 1% penicillin/streptomycin supplemented with 5 ng/mL basic fibroblast growth factor (bFGF, Invitrogen). Cells were maintained at 37°C in a water-saturated atmosphere containing 5% CO_2 in air. To induce differentiation, primary myoblasts at 80% confluence were placed in Differentiation Medium (DM) consisting of Ham's F10 with 10% horse serum and 1% penicillin/streptomycin.

2.9 | Proliferation assay and fusion index measurement

Primary myoblast proliferation was assessed as described in Oliver et al.[24] Cells were seeded at 2500 cells per well in GM in 96-well microtiter plates and fixed at regular 24 hours periods before methylene blue staining and measured at A_{590nm} using an ELISA plate reader (FLUOstar Omega; BMGLabtech, Ortenberg, Germany). Point 0 hour of proliferation does not correspond to plating but to 6 hours post-plating. Fusion index measurement was performed by immunofluorescence as previously described.[25] Cells were fixed in 4% paraformaldehyde for 10 minutes and permeabilized with 0.1%Triton X-100-PBS for 30 minutes at 4°C. The cells were washed three times in PBS 1X and saturated for 1 hour at room temperature using PBS with 20% goat serum. Then, the cells were stained with the primary antibody 1:500 in PBS-BSA 4% (Anti-MyHC Class II antibody, Abcam) overnight in a humid atmosphere at 4°C. Cells were washed three times for 5 minutes with 0.01% Tween 20-PBS and incubated with the Alexa-Fluor conjugated secondary antibody (1:1000) and DAPI (1:1000) in PBS-BSA 4% for 15 minutes at 37°C in a humid atmosphere. Images were acquired with a Leica DMI6000B inverted epifluorescence microscope using the MetaMorph software (Molecular Devices, Sunnyvale, USA). Fusion index was calculated by dividing the number of myonuclei contained in MyHC-expressing myotubes by the total number of myonuclei (ImageJ software).

2.10 | Metabolic analyses

For intraperitoneal glucose tolerance test (IPGTT), 16 hours-fasted mice were injected with 20% D-glucose (2 mg/g body weight). Glucose levels were measured using a glucose meter (OneTouch Ultra) from tail blood at 0, 15, 30, 60, and 120 minutes after glucose injection.

2.11 | Skeletal muscle enzymatic activities

Lactate dehydrogenase (LDH) and isocitrate dehydrogenase (ICDH) were measured from a 5% (w/v) muscle (quadriceps or *gastrocnemius*) homogenate in pH 8.0 buffer (250 mM sucrose, 2 mM EDTA, 10 mM Tris). The frozen muscle was crushed in the buffer on ice with an ultra-turax. After centrifugation at 6000 rpm for 15 minutes at 4°C, the supernatants were removed

and stored on ice until the enzymatic activities were measured using the Konelab 30 controller (Thermo Scientific). The measurement of the LDH and ICDH activities at A_{340nm} was based on the NADH disappearance or production, respectively. The reactions were done in LDH buffer (Triethanolamine 50 mM/EDTA 5 mM/Pyruvate de sodium 2 mM/NADH 0.234 mM/pH 7.5) or ICDH buffer (Na2HPO4 36.1 mM/MgCl2 0.5 mM/Triton 0.05%/NADP 0.334 mM/Isocitrate 1.29 mM/pH 7.3)

2.12 | Statistical analyses

Unless otherwise stated, results are expressed as mean ± SEM. One-way ANOVA was performed to examine the effect of genotype (WT vs genotype) on each parameter. Statistical significance was set at $P < .05$. A minimum of three replicates were performed for each experimental condition.

3 | RESULTS

3.1 | Generation of *Gasp-2* transgenic mouse lines

We constructed a transgene expressing mouse *Gasp-2* cDNA under the control of a CMV promoter to create mice overexpressing ubiquitously *Gasp-2*. Two independent *Tg(Gasp-2)* lines were successfully established and named Tg(*Gasp-2.2*) and Tg(*Gasp-2.9*). Transgene copy number was estimated by semi quantitative real-time PCR using *Ccr5* gene as an endogenous reference to normalize the amount of chromosomal

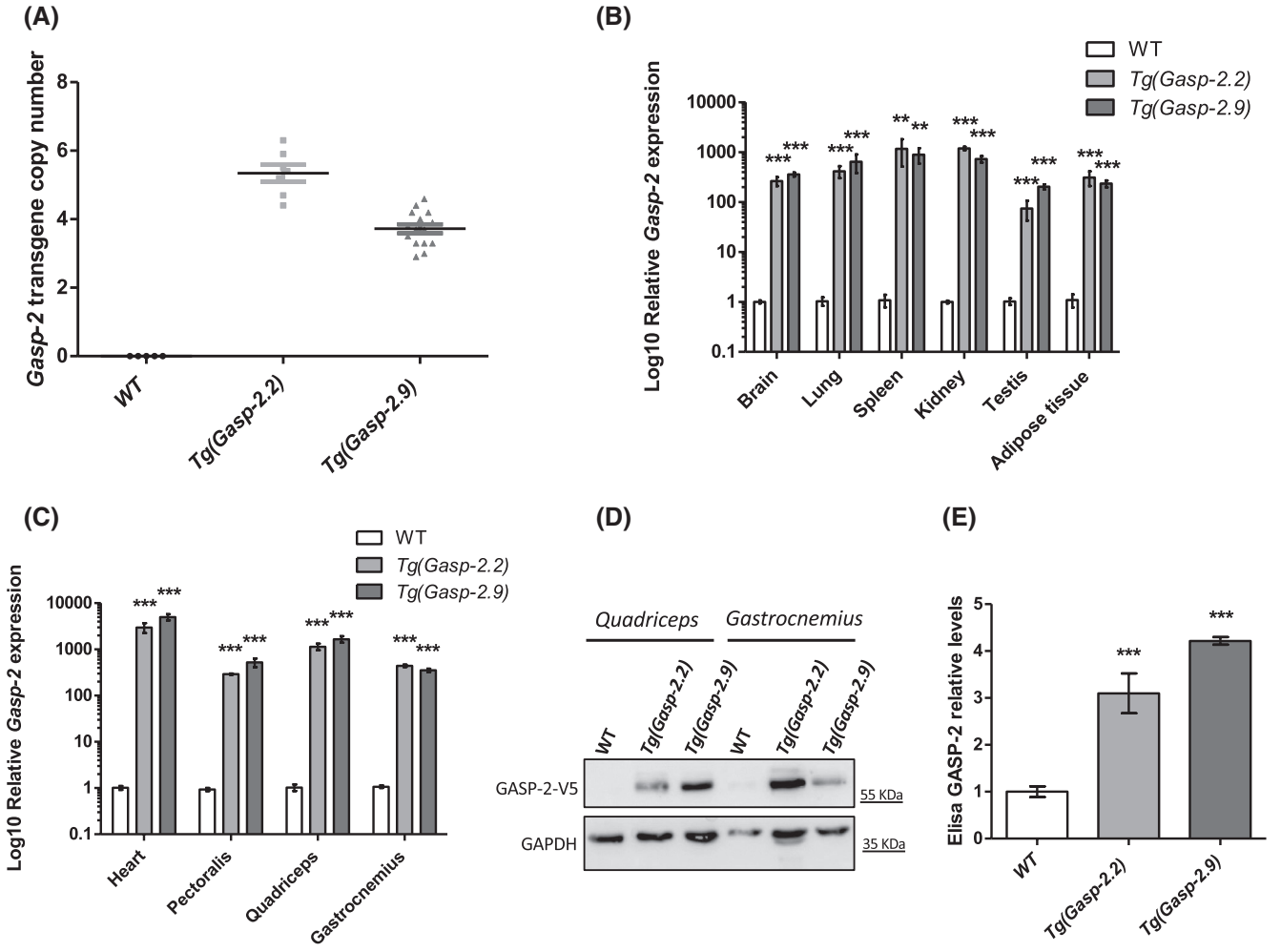

FIGURE 1 Generation of *Gasp-2* transgenic mouse lines. A, *Real*-time PCR-*based* transgene copy number determination of wilt-type (WT) (n > 5), *Tg(Gasp-2.2)* (n > 5) and *Tg(Gasp-2.9)* mice (n > 5). B, Relative mRNA expression levels of *Gasp-2* were measured by quantitative PCR in brain, lung, spleen, kidney, testis, and adipose tissues and (C) heart, *Pectoralis*, quadriceps, and *Gastrocnemius* from WT (white), *Tg(Gasp-2.2)* (light grey), and *Tg(Gasp-2.9)* (dark grey) (n = 10). D, Western blot analysis of transgene-driven GASP-2 protein expression with an anti-V5 antibody. Total proteins were extracted from quadriceps and *Gastrocnemius* from WT and *Tg(Gasp-2)* mice. GAPDH was used as a loading control signal of three distinct experiments. E, Concentrations of serum GASP-2 were determined in sandwich ELISA from WT and *Tg(Gasp-2)* lines (n = 4). Data are shown as means ± SEM; One-way ANOVA was performed (WT vs genotypes) (***P value < .001)

DNA. The homozygous *Tg(Gasp-2.2)* mice harbored ~ six copies of the transgene, while the Tg(*Gasp-2.9*) mice had ~ four copies (Figure 1A). The copy number was stable within all subsequent generations. The two *Tg(Gasp-2)* lines displayed a strong expression of *Gasp-2* (100- to 10 000-fold compared to WT) in various tissues (Figure 1B) and muscles (Figure 1C). The transgene-driven GASP-2 protein expression was further analyzed by western blotting with an anti-V5 antibody (Figure 1D), confirming the GASP-2 overexpression in both lines. As GASP-2 is a secreted protein, we measured its amount in serum and showed a 3-fold overexpression of GASP-2 in Tg(*Gasp 2.2*) mice and 4-fold in Tg(*Gasp 2.9*) mice (Figure 1E).

3.2 | Overexpression of *Gasp-2* leads to a hypermuscular phenotype due to hypertrophy without hyperplasia

Mice overexpressing *Gasp-2* have a higher overall weight compared to WT mice from weaning to 90 days (Figure 2A). Compared to 3-month-old WT mice, the *Tg*(*Gasp-2.2*) and *Tg*(*Gasp-2.9*) animals exhibit a total body weight increase of 11.5% and 13%, respectively. Furthermore, the overexpression of *Gasp-1*, the paralog of *Gasp-2,* or the knock-out of *Mstn*, the targeted gene by *Gasp-2*, lead to an overall weight increase of 15% and 28% in mice, respectively (Figure 2B). This gain is associated with an increase in skeletal muscle

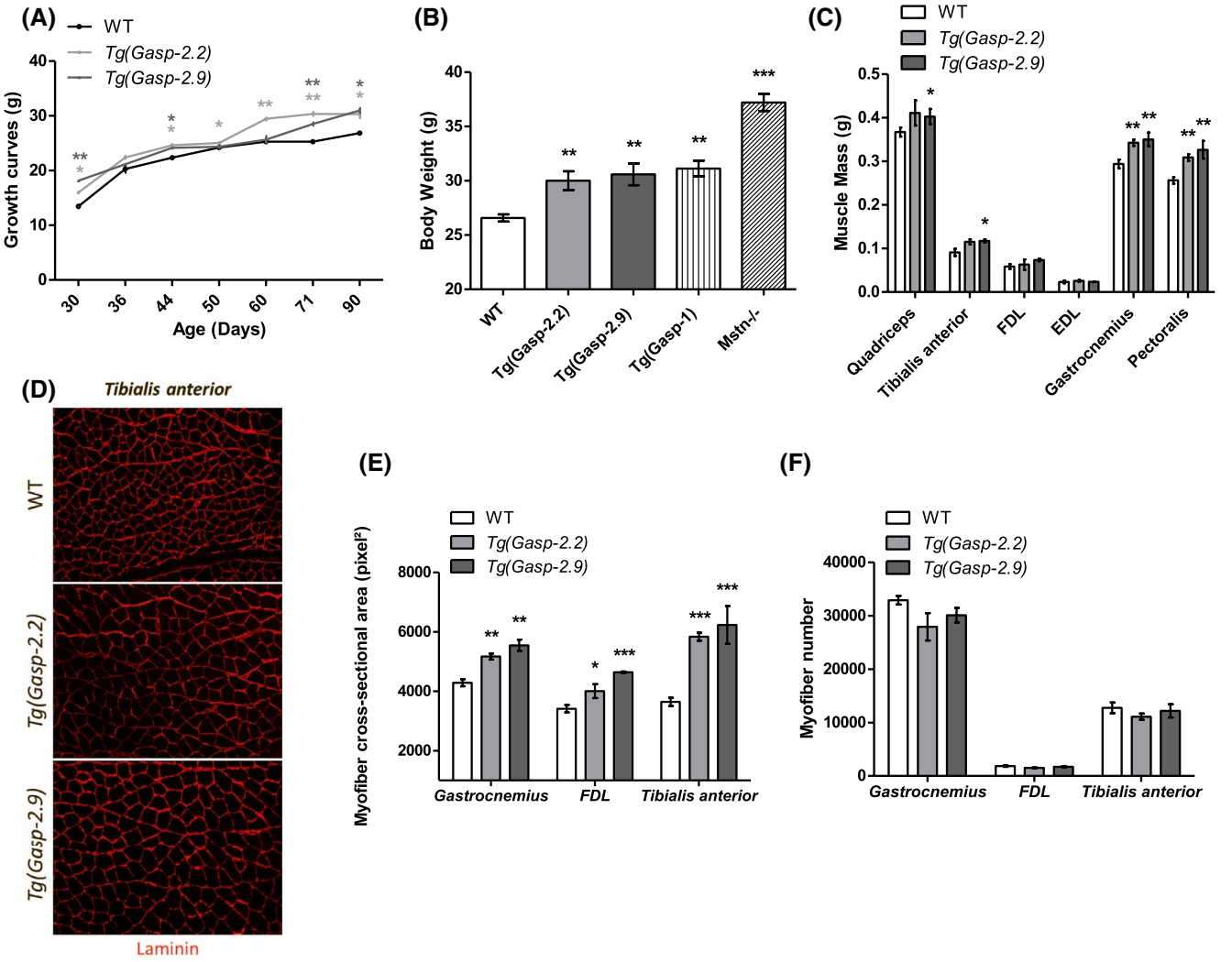

FIGURE 2 Characterization of skeletal muscles from *Tg(Gasp-2)* mice. A, Total body weight of WT (black, n = 10), *Tg(Gasp-2.2)* (light grey, n = 10), and *Tg(Gasp-2.9)* (dark grey, n = 10) were measured from 30 to 90 days old. B, Total body weight of 3-month-old mice (n = 15 mice/genotype). C, Muscles of 3-month-old mice were harvested and weighed. D, Representative cryosections of *Tibialis anterior* from 3-month-old WT and *Tg(Gasp-2)* mice. Laminin (red) staining showed basal lamina of myofibers. E, Mean myofiber cross-sectional areas and (F) mean myofiber numbers of *Gastrocnemius*, *Flexor Digitorum Longus* (FDL) and *Tibialis anterior* muscle from 3-month-old WT and *Tg(Gasp-2)* mice (n = 10 mice/genotype). Data are shown as means ± SEM; One-way ANOVA was performed (WT vs genotypes) (**P* value < .05; ***P* value < .005; ****P* value < .001). Benferroni posttest was used for the weight curve to include a correction for repeated measures

mass of *Tg(Gasp-2)* lines (*gastrocnemius*, *tibialis anterior*, *pectoralis,* and quadriceps) (Figure 2C). To confirm whether this muscle phenotype is due to hypertrophy and/or hyperplasia, histological analyses were carried out on three muscles (*tibialis anterior*, *soleus,* and *Gastrocnemius)* (Figure 2D-F). Muscle cross sections of *Tg(Gasp-2.2) and Tg(Gasp-2.9)* mice immunostained with an anti-laminin antibody show an increase of myofiber cross-sectional area (CSA) compared to the WT mice, independently of the muscle type (Figure 2D,E). However, no significant difference in muscle fibers number was observed between WT and *Tg(Gasp-2)* mice (Figure 2F). This phenotype is found preserved at 6 months (data not shown). These results show that the overexpression of *Gasp*-2 leads to a myofiber hypertrophy without hyperplasia, as we have previously observed in *Tg(Gasp-1)* mice.

3.3 | *Tg(Gasp-2)* mice display a switch from slow- to fast-twitch myofibers.

It has been shown that *Mstn*$^{-/-}$ mice present a switch from slow- to fast-twitch myofibers. We checked whether the *Gasp-2* overexpression leads to a change in the myofiber type proportion in two different muscle. We measured the overall activity of isocitrate dehydrogenase ICDH and lactacte dehydrogenase LDH from extracts of *gastrocnemius* and quadriceps of 3-month-old animals (Figure 3A,B). Like *Mstn*$^{-/-}$ mice, *Tg(Gasp-2.2)* and *Tg(Gasp-2.9)* mice show a decrease in ICDH activity compared to WT (Figure 3A). In opposite, *Tg(Gasp-1)* mice do not present this ICDH decrease but exhibit a decrease in LDH activity (Figure 3A,B). Quantification of the different type of myofibers tends to show a decrease in the percentage of type I myofibers and

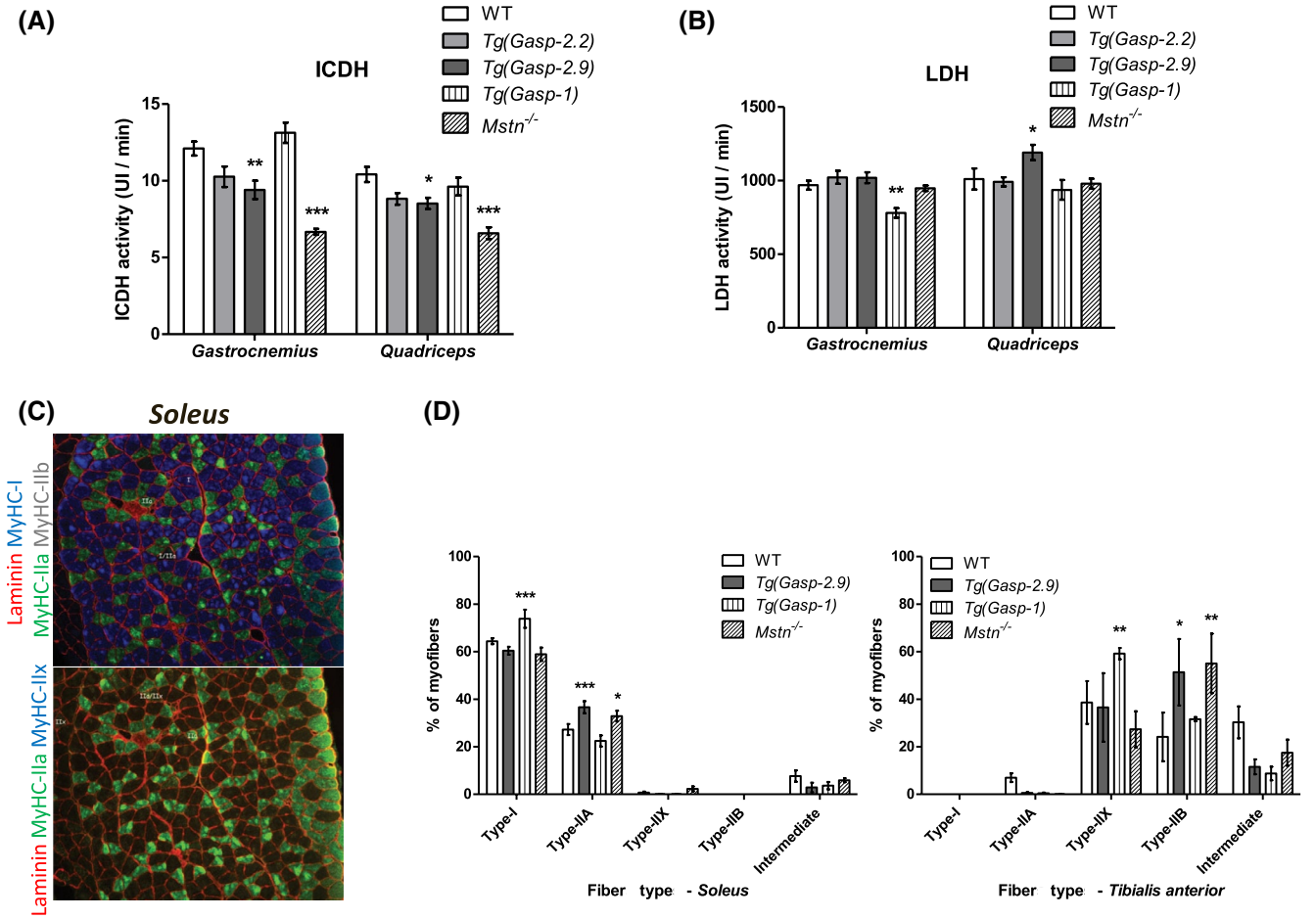

FIGURE 3 Skeletal muscle fiber type distribution from *Tg(Gasp-2)* mice. A, Isocitrate dehydrogenase (ICDH) and (B) Lactate dehydrogenase (LDH) were measured from *Gastrocnemius* or quadriceps muscle from 3-month-old WT, *Tg(Gasp-2.2)*, *Tg(Gasp-2.9)*, *Tg(Gasp-1),* and *Mstn*$^{-/-}$ mice (n = 10 mice/genotype). The measurement of the LDH and ICDH activities at A_{340nm} was based on the NADH disappearance or production, respectively. C, Representative cryosections of *Soleus* from 3-month-old WT immunostained with an antibody cocktail. D, Percentage of fibers type distribution in the *Soleus* and *Tibialis Anterior*, realized by semiautomatic image analysis Visilog software, using the double laminin/myosin labelling (n > 5 mice/genotype). Data are shown as means ± SEM; One-way ANOVA was performed (WT vs genotypes) (**P* value < .05; ***P* value < .005; ****P* value < .001)

a significant increase of type IIA myofibers in *soleus* of *Tg(Gasp-2)* line (Figure 3C,D). A similar result was observed in *Mstn*$^{-/-}$ mice but not in *Tg(Gasp-1)* mice which showed a significant increase in type I fibers and decrease in type IIA myofibers (Figure 3D). We observed the same switch from slow- to fast-twitch in the *tibialis anterior* muscle (Figure 3D).

3.4 | Overexpression of *Gasp-2* leads to an increase of myonuclei accretion during the first 3 postnatal weeks

Muscular hypertrophy could be associated to the addition of new nuclei from activated satellite cells within the myofiber and/or to the increased rate of protein synthesis. We therefore analyzed the muscle phenotype of 3-week-old mice, just after the myonuclear accretion phase. The *Tg(Gasp-2.2)* and *Tg(Gasp-2.9)* mice already show an increase of muscle mass due to a myofiber hypertrophy without hyperplasia (Figure 4A-C). The number of myonuclei per myofiber was increased in *tibialis anterior* in *Tg(Gasp-2)* lines, demonstrating a higher myonuclear accretion (Figure 4D). The pool of Pax7^{+} positive satellite cells are not affected after this myonuclear accretion phase in overexpressing *Gasp-2* skeletal muscles (Figure 4E).

3.5 | Overexpression of *Gasp-2* in *Tg(Gasp-2)* primary myoblasts enhances cell proliferation and differentiation

To investigate the molecular mechanisms regulating muscle mass in both *Tg(Gasp-2)* lines which present the same phenotype, myoblasts derived from *Tg(Gasp-2.9)* satellite cells were isolated. We showed that *Tg(Gasp-2.9)* myoblasts overexpressed *Gasp-2* (a 100-fold change) at 48 hours of proliferation without affecting the *Gasp-1* and *Mstn* expression (Figure 5A). This result is quite surprising since we previously demonstrated that the *Tg(Gasp-1)* myoblasts showed an upregulation of *Mstn*. *Tg(Gasp-2.9)* cells were assessed for rate of proliferation and showed a faster proliferation (Figure 5B), associated with a decrease of pSMAD2/3 (Figure 5C). These results revealed that *Gasp-2* overexpression inhibited TGF-β pathway (including *Mstn*) which normally activated SMAD2/3 phosphorylation

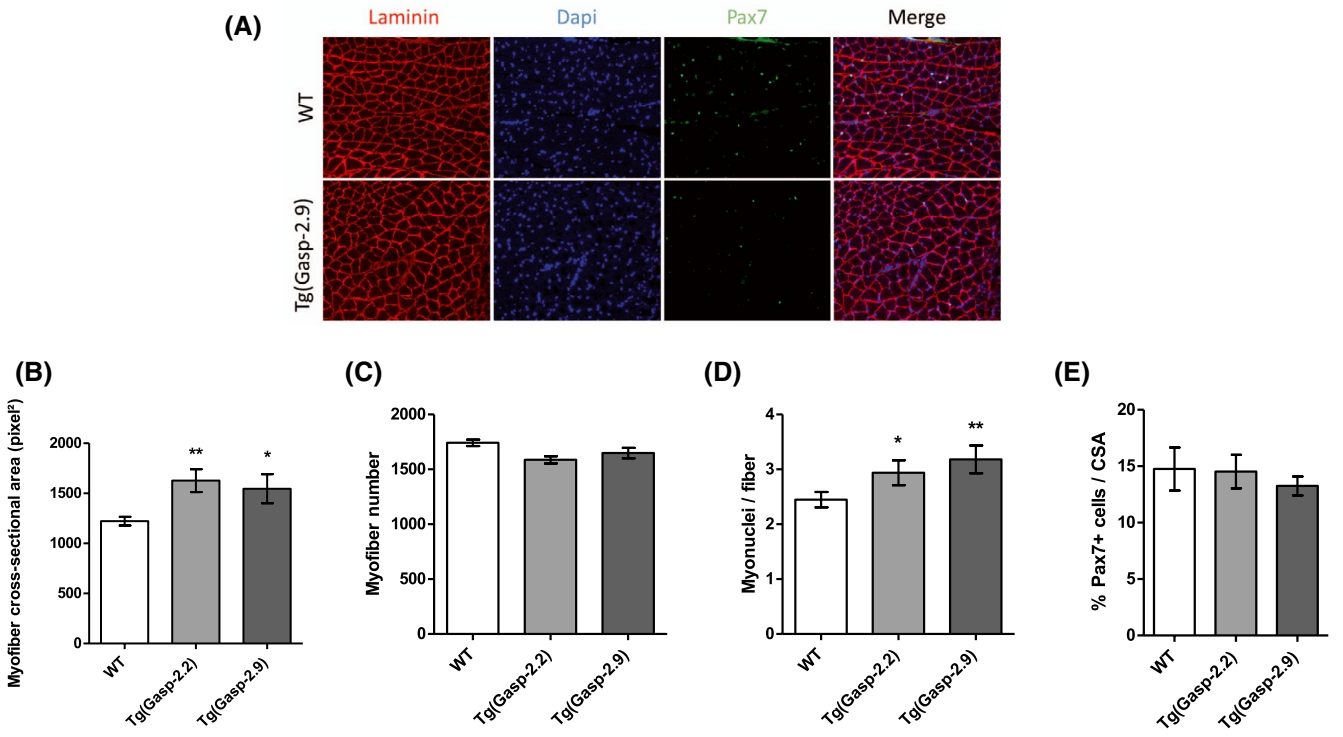

FIGURE 4 Characterization of skeletal muscles after myonuclear accretion phase. A, Representative cryosections of *Tibialis Anterior (TA)* muscle from 3-week-old WT and *Tg(Gasp-2.9)* mice immunostained for laminin (red), Pax7 (green), and DAPI (blue). B, Mean myofiber cross-sectional areas and (C) mean myofiber numbers of *TA* muscle from 3-week-old WT and *Tg(Gasp-2)* mice (n > 5 mice/genotype). D, Quantification of the number of myonuclei per fiber in *TA* from 3-week-old WT and Tg(Gasp-2) mice and (F) percentage of satellite cells (Pax7^{+}) per cross-sectional area (n > 5 mice/genotype). A nucleus was identified as myonucleus if one of the following criteria is observed: (i) the nucleus was located within the laminin boundary, (ii) the nucleus is at the inner periphery of the fibre (laminin) or (iii) >50% of the surface of the nucleus was within the laminin boundary. Data are shown as means ± SEM; One-way ANOVA was performed (WT vs genotypes) (*P value < .05; **P value < .005)

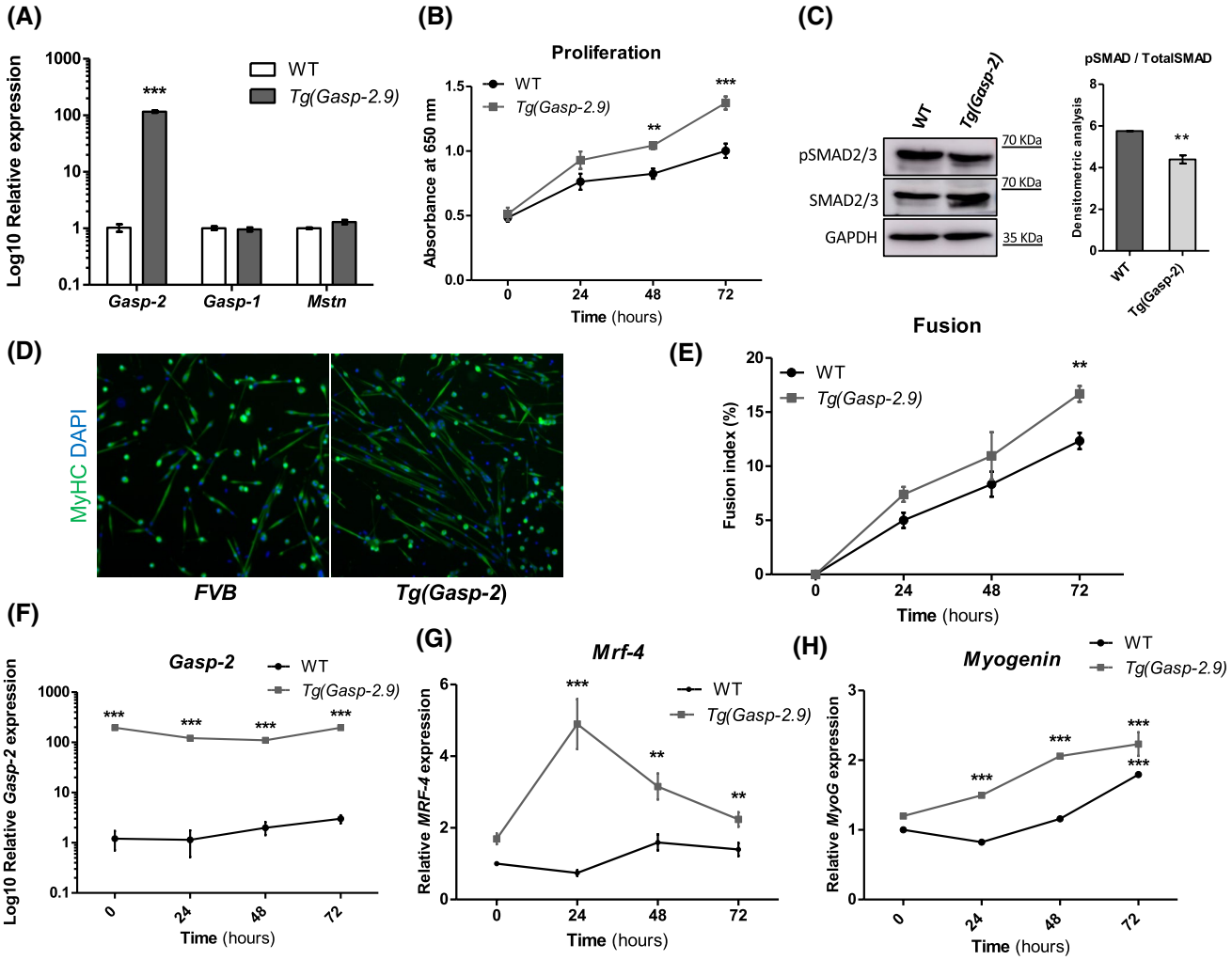

FIGURE 5 Overexpression of *Gasp-2* in *Tg(Gasp-2)* primary myoblasts. A, Relative mRNA expression levels of *Gasp-2*, *Gasp-1,* and *myostatin* (*Mstn*) were measured by quantitative PCR of WT and *Tg(Gasp-2.9)* myoblasts grown under proliferating conditions for 48 hours. B, WT and *Tg(Gasp-2.9)* primary myoblasts were plated at 2500 cells per well and grown in growth medium for a period of 72 hours. Proliferation was measured by Methylene Blue assay (n = 5 independent experiments). C, Immunoblot analysis of pSMAD2/3 expression of WT and *Tg(Gasp-2.9)* myoblasts grown under proliferating conditions for 48 hours. Nitrocellulose membranes were also probed with anti-GAPDH antibody and anti-SMAD 2/3 total to show equal loading of samples. D, WT and *Tg(Gasp-2.9)* myotubes were immunostained for MyHC protein at 72 hours after induction of differentiation. The cells were plated before differentiation at confluence (20 000 cells/cm^2) and not at subconfluence to avoid seeing a proliferation impact on differentiation. E, Fusion indexes during 72 hours of WT and *Tg(Gasp-2.9)* myoblasts differentiation were determined from DAPI/Myosin staining (n = 3 independent experiments). F, Relative mRNA expression levels of *Gasp-2*, (G) *Mrf-4* and (H) Myog were measured by quantitative PCR from 0 to 72 hours of differentiation in WT and *Tg(Gasp-2)* primary myotubes (n = 3 independent experiments). Data are shown as means ± SEM; One-way ANOVA was performed (WT vs genotypes) (***P* value < .005; ****P* value < .001)

to inhibit proliferation. Using myosin immunostaining, we observed after 72 hours of differentiation that *Tg(Gasp-2.9)* myoblasts form larger myotubes compared to WT (Figure 5D). Fusion index of *Tg(Gasp-2.9)* myotubes is increased, leading to a higher differentiation rate (Figure 5E). In addition, the expression of the two myogenic factors of the terminal differentiation, *Mrf-4* and *myogenin* (Myog), normally inhibited by *Mstn*, are more expressed in *Tg(Gasp-2.9)* cells throughout the time course of differentiation (Figure 5F-H).

To obtain more insight into molecular characterization, we performed a gene expression array analysis during proliferation of 43 genes involved in muscle development. Among the 43 genes, 10 genes were upregulated and 5 were downregulated (Table 1). *Gasp-2* expression was increased more than 247-fold in the *Tg(Gasp-2)* myoblasts compared to the WT, confirming that *Gasp-2* overexpression was significant in *Tg(Gasp-2)* satellite cell-derived primary myoblasts. We also found that *Myf6, MyoG* and *Inhba* (Inhibin beta A chain) were upregulated in *Tg(Gasp-2)* cells. In contrast, the *Ltbp3* (Latent transforming growth factor beta binding protein 3) gene, another TGF-β inhibitor was downregulated in *Tg(Gasp-2)* myoblasts (Table 1).

TABLE 1 Relative expression levels of deregulated genes in *Tg(Gasp-2)* myoblasts

	Gene ID	Gene symbol	Description	Fold changes	*P* value
Upregulated	215001	*Gasp-2*	*Growth and differentiation factor-associated serum protein-2*	247.81	0.0014
	16323	*Inhba*	*Inhibin Beta-A*	2.81	0.00364
	16322	*Inha*	*Inhibin alpha*	2.74	0.00209
	21809	*Tgfb3*	*Transforming growth factor B 1*	2.48	0.0316
	21808	*Tgfb2*	*Transforming growth factor B 1*	2.33	0.0411
	17878	*Myf6*	*Myogenic factor 6*	2.01	0.0134
	17928	*Myog*	*Myogenin*	2.01	0.00919
	18121	*Nog*	*Noggin*	1.98	0.0136
	12111	*Bng*	*Biglycan*	1.86	0.00549
	12667	*Chrd*	*Chordin*	1.79	0.0573
Downregulated	14560	*Gdf10*	*Growth and differentiation factor 10*	−1.77	0.850
	18505	*Pax3*	*Paired box protein 3*	−1.96	0.134
	17927	*Myod1*	*Myod1*	−2.06	0.228
	16998	*Ltbp3*	*Latent TGF-b binding protein 3*	−2.21	0.210
	18119	*Nodal*	*Nodal*	−3.59	0.648

Note: List of upregulated or downregulated genes by more than 1.5-fold in *Tg(Gasp-2)* primary myoblasts compared with WT primary myoblasts during proliferation. One-way ANOVA was performed (WT vs genotypes).

TABLE 2 Relative expression levels of deregulated genes in *Tg(Gasp-2)* mice

				Stages			
				Embryonic stage—E9.5		Fœtal stage—E14.5	
	Gene ID	Gene symbol	Description	Fold changes	*P* value	Fold changes	*P* value
Upregulated	215001	*Gasp-2*	*Growth and differentiation factor-associated serum protein-2*	22.16	.02474	19.99	.00717
	14561	*GDF-11*	*Growth differentiation factor 11*	2.88	.00874	2.22	.0142
	18505	*Pax3*	*Paired box protein 3*	3.07	.0502	3.76	.0368
	18509	*Pax7*	*Paired box protein 7*	2.63	.0282	3.06	.0254
	12159	*Bmp4*	*Bone morphogenetic protein 4*	2.82	.0263	2.38	.0393
Downregulated	215001	*Gasp-1*	*Growth and differentiation factor-associated serum protein-1*	−14.12	.0373	−2.013	.0381
	14313	*Fst*	*Follistatin*	−2.26	.0423	−2.12	.0454
	13179	*Dcn*	*Decorin*	−12.04	.00482	−6.11	.00274
	108075	*Ltbp4*	*Latent TGF-b binding protein 4*	−3.29	.0522	−1.78	n.s
	12111	*Bgn*	*Biglycan*	−5.22	.0323	−2.95	.0189
	16324	*Inhbb*	*Inhibin beta-b*	−5.75	.0180	−2.04	n.s
	16326	*Inhbc*	*Inhibin beta-c*	−8.59	.00849	−4.47	n.s
	12156	*Bmp3*	*Bone morphogenetic protein 3*	−6.47	.0361	2.487	.00647

Note: Fold change of genes involved in the TGF-β signaling pathway in *Tg(Gasp-2)* mice are compared with WT mice at embryonic stages E9.5 and E14.5. One-way ANOVA was performed (WT vs genotypes) n.s., non-significant.

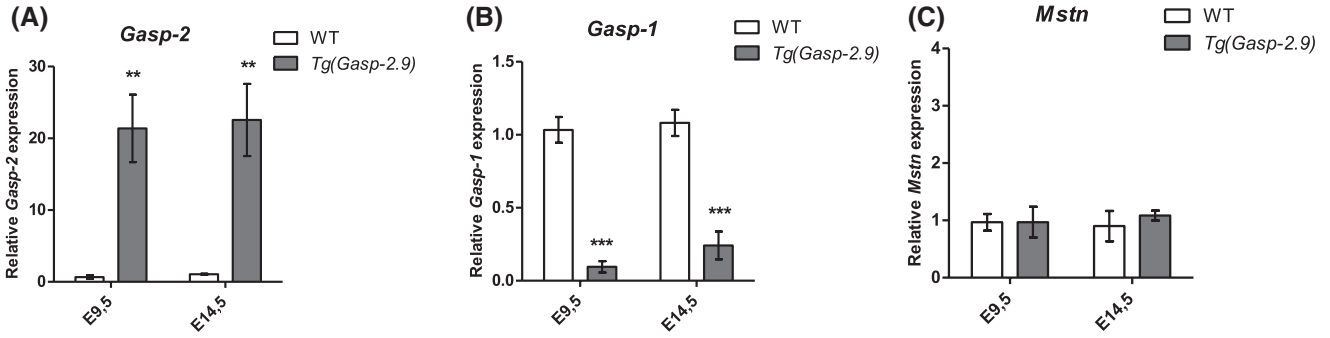

FIGURE 6 Relative expression levels of deregulated genes in *Tg(Gasp-2)* embryos. Relative mRNA expression levels of (A) *Gasp-2*, (B) *Gasp-1,* and (C) *myostatin* were measured by qRT-PCR at embryonic stages E9.5 (primary myogenesis) and E14.5 (secondary myogenesis) from WT and *Tg(Gasp2.9)* embryos. Data are shown as means ± SEM; One-way ANOVA was performed (WTvs genotypes) (***P* value < .005; ****P* value < .001)

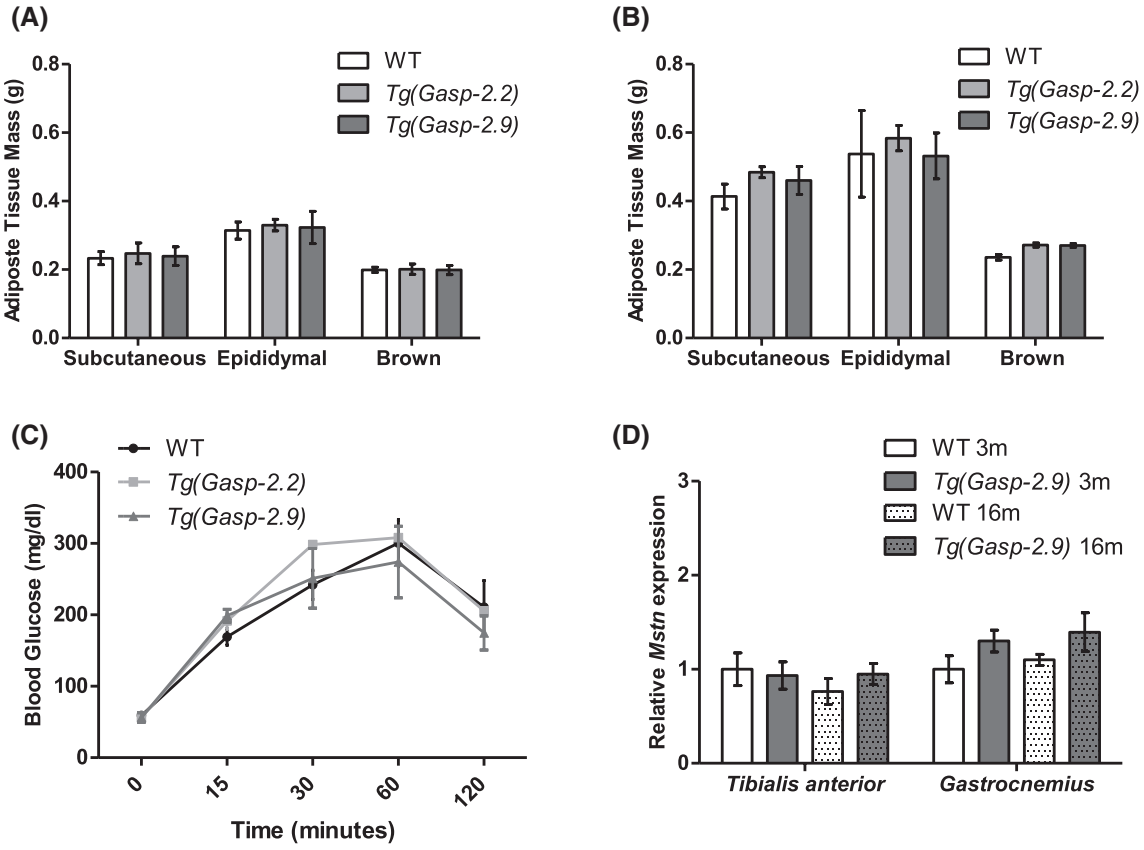

FIGURE 7 Adipose phenotype in *Tg(Gasp-2)* mice. Adipose tissue mass from (A) 3-month-old and (B) 16-month-old WT and *Tg(Gasp-2)* mice. C, Intraperitoneal glucose tolerance test from overnight-fasted mice, injected with glucose (2 mg/g body weight). Blood glucose levels were monitored at 0, 15, 30, 60, and 120 minutes after glucose injection of 16-month-old mice. D, Relative mRNA expression levels of *myostatin* (Mstn) were measured by quantitative PCR of WT and *Tg(Gasp-2.9)*. Data are shown as means ± SEM; One-way ANOVA was performed (WT vs genotypes)

3.6 | Deregulated expression of TGF-β and their inhibitors during primary and secondary myogenesis in *Tg(Gasp-2)* mice

Understanding the absence of hyperplasia in *Gasp-2* overexpressing mice requires to investigate gene expression levels during primary (at E9.5 embryonic stage) and secondary myogenesis (at E14.5 fetal stage). We found a 20-fold overexpression of *Gasp-2* at both stages (Table 2 and Figure 6A). Interestingly unlike the *Tg(Gasp-1)* mice, the *Tg(Gasp-2)* animals do not present variation in *Mstn* expression but exhibit at these stages a 2- to 3-fold upregulation of *Gdf11*, a gene closely related to *Mstn* known to

regulate anterior/posterior axial patterning (Table 2 and Figure 6B). Moreover, *Tg(Gasp-2)* mice show a 2- to 14-fold downregulation of several *Mstn* inhibitors such as *Gasp-1*, *Fst*, *Dcn, and Ltbp4* at embryonic stages (Table 2 and Figure 6C). Our findings highlighted a gene expression regulatory network of TGF-β members and their inhibitors during primary and secondary myogenesis. This transcriptional deregulation could be responsible for the absence of hyperplasia by counteracting the effect of *Gasp-2* overexpression.

3.7 | Overexpressing *Gasp-2* mice do not present an adipose and insulin resistance phenotype

We have previously shown that the *Tg(Gasp-1)* mice gained weight with age due to an increase in fat mass, hyperglycemia, and insulin resistance and found that all these symptoms are dependent of an upregulation of *Mstn*.[20] At 3 months, the *Tg(Gasp-2.2)* and *Tg(Gasp-2.9)* mice do not present changes in adipose tissue mass (subcutaneous, epididymis and brown) compared to controls (Figure 7A). Unlike *Tg(Gasp-1)* animals, the 16-month-old *Tg(Gasp-2)* mice show no increase in their fat mass (Figure 7B). In IPGTT, there was no difference in glucose clearance between old mutant and WT mice (Figure 7C). Molecular analyses revealed no upregulation of *Mstn* in young and aged *Tg(Gasp-2)* muscles (Figure 7D).

4 | DISCUSSION

In this paper, we studied the cellular and molecular mechanisms underlying the muscle phenotype in a mouse model overexpressing GASP-2, a *Mstn* inhibitor, to investigate a potential

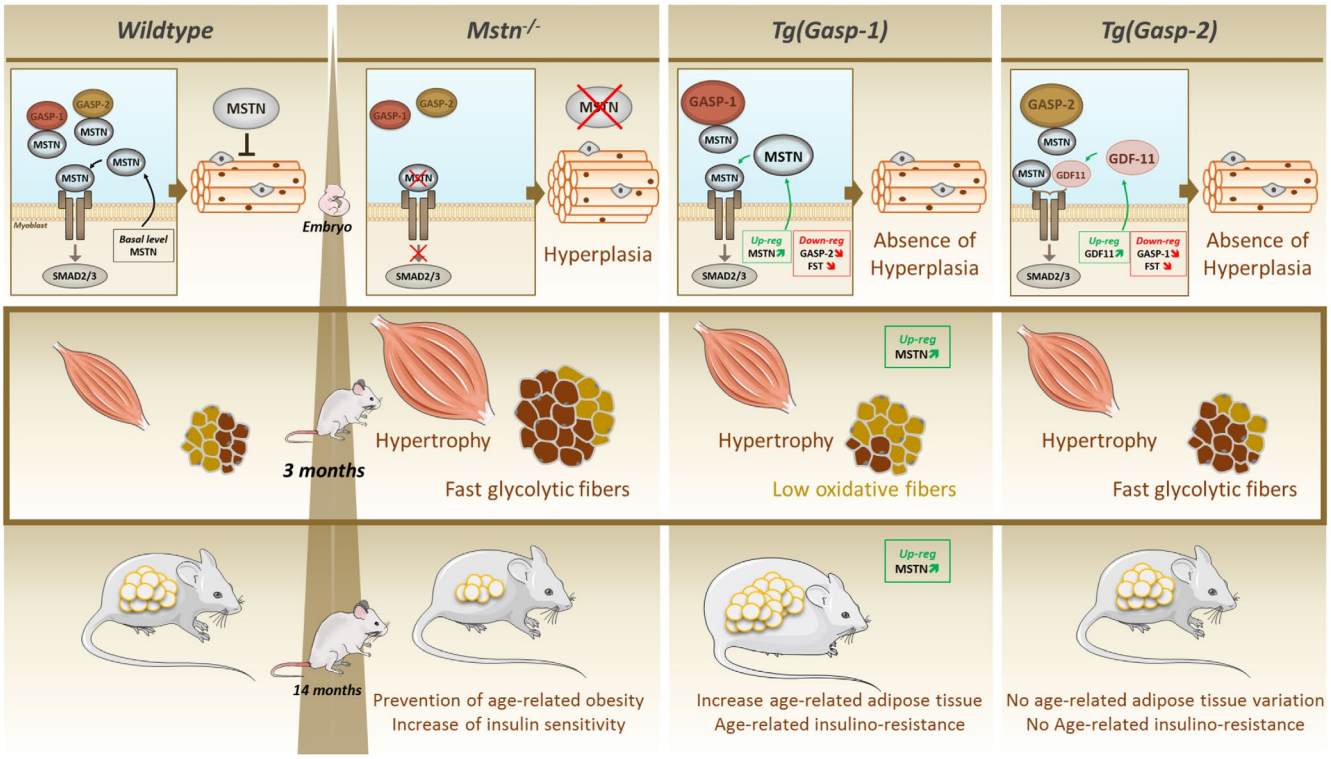

FIGURE 8 A model highlighting the functional duality of GASP-1 and GASP-2 for myostatin inhibition. Molecular and/or phenotypic analyses after *myostatin* knockout ($Mstn^{-/-}$ mice), *Gasp-1* overexpression (*Tg(Gasp-1)*), and *Gasp-2* overexpression (*Tg(Gasp-2)*) in adult stage—3 months—(*middle part*), in embryonic stage (*upper part*) and aged stage—14 months—(*lower part*). In comparison to WT, $Mstn^{-/-}$ mice exhibit an increase in muscle mass due to both hyperplasia and hypertrophy of myofibers, and a decrease in fat mass with age. Phenotypic analysis revealed at 3 months that both *Gasp-1* and *Gasp-2* overexpression in adult mice leads to an increase in muscle mass only due to myofiber hypertrophy without hyperplasia. *Tg(Gasp-2)* mice, like $Mstn^{-/-}$ mice, display a switch from slow- to fast-twitch myofibers, while *Tg(Gasp-1)* mice exhibit an opposite switch. Interestingly, at 14 months of age, only the *Tg(Gasp-1)* mice develop most of the symptoms associated with a metabolic syndrome, resulting in an upregulation of *Mstn*. Molecular studies show, at embryonic stage (stage of hyperplasia formation), that (i) overexpression of *Gasp-1* leads to *upregulation* of *Mstn* and downregulation of *Gasp-2* and *follistatin* (FST, a myostatin inhibitor) whereas (ii) overexpression of *Gasp-2* results in *upregulation* of *GDF-11* (a MSTN-homologous protein) and a downregulation of *Gasp -1* and *Fst*

new therapeutic approach for muscle atrophy. Although its paralog, GASP-1, was a good candidate because it led to a hypermuscular phenotype when overexpressed, age-related metabolic defects are also observed in *Tg(Gasp-1)* mice.[20] To date, only the phenotypic study of *Gasp-2* deficient mice associates *in vivo* GASP-2 with a context of muscle.[26] These knock-out mice develop muscle atrophy and have defects in myofiber regeneration. Here, we generated and characterized two independent lines overexpressing *Gasp-2*, *Tg(Gasp-2.2)* and *Tg(Gasp-2.9)*, to better understand the functions of GASP-2 and evaluate its therapeutic potential. We showed that these mice present an increase of skeletal muscle mass due to myofiber hypertrophy at 3 months, still observed at 6 months. This increase is similar to that seen for the *Tg(Gasp-1)* mice and is less than the observed muscle increase of the *Mstn*-null mice. We demonstrated that this hypertrophy was accompanied by an increase of myonuclear accretion during the first 3 postnatal weeks. In accordance with these results, we showed that overexpressing *Gasp-2* primary myoblasts proliferated faster and myonuclei average per myotube was increased during differentiation. Thus, overexpression of *Gasp-2* could result in accelerated regeneration during muscle injury.

Unlike $Mstn^{-/-}$ mice, no muscle hyperplasia was observed in *Tg(Gasp-2)*. We previously observed this absence of hyperplasia in the *Tg(Gasp-1)* line and have shown an upregulation of *Mstn* at the embryonic stages, which counterbalances the effect of *Gasp-1* overexpression during the early phases of myogenesis.[21] Interestingly, we did not find a *Mstn* upregulation in the *Tg(Gasp-2)* embryos but an upregulation of *Gdf-11*, a gene closely related to *Mstn* known to regulate anterior/posterior axial patterning.[27] Recent studies showed that GDF-11 could inhibit skeletal muscle development similar to *Mstn*.[28-30] Differentially upregulation of *Mstn* or *Gdf-11* in *Gasp-1 or Gasp-2* overexpressing models could be explained by a different affinity between GASP proteins with *Mstn* or GDF-11. Indeed, Kondás et al[15] and Walker et al[31] showed that in vitro, GASP-1 is approximately 100 times more affine for *Mstn* than GASP-2 and GASP-2 would have a better affinity for GDF-11.[15,31] Our in vivo data are consistent with these results and are reinforced by the presence of an up-regulation of *Mstn* in the *Tg(Gasp-1)* mice, while *Gdf-11* is up-regulated in *Tg(Gasp-2)* line. In addition, *Tg(Gasp-2)* mice present a downregulation of several *Mstn* inhibitors such as *Gasp-1*, *Follistatin, decorin, and Ltbp3* at embryonic stage. A similar result was observed in *Tg(Gasp-1)* mice, with a downregulation of *Gasp-2*, *Follistatin, and Ltbp1* expression. Our findings highlighted a gene expression regulatory network of TGF-β members and their inhibitors in muscle, responsible for the absence of hyperplasia by counteracting the effect of *Gasp-2* overexpression.

Unlike the *Tg(Gasp-1)* mice,[21] GASP-2 overexpression did not lead to metabolic defects with age. In addition, the *Tg(Gasp-2)* mice display, like the $Mstn^{-/-}$ mice, a switch from slow- to fast-twitch myofibers whereas *Tg(Gasp-1)* mice exhibit a switch from fast- to slow-twitch myofibers. Altogether, the difference of the phenotypes observed between the *Tg(Gasp-1)* and *Tg(Gasp-2)* lines could be explained at the molecular level by the induction or not of *Mstn* upregulation as shown in Figure 8. Our results suggested that the GASP-2 protein might be a better candidate to target *Mstn* -signaling pathway without affecting the metabolism. To further develop the potential of GASP-2 as a therapeutic treatment, it would be interesting to get any functional assessment of muscle contractile activity or of muscle regenerative potential.

ACKNOWLEDGMENTS

We are indebted to Dr. J.L. Vilotte and Dr. B. Passet (UMR 1313 GABI, Jouy-en-Josas) for their help in generating the transgenic mice. We also thank K. Pasquier from the plateform BISCEm (animal facility) for her technical help with animals. This project was co-financed by the European Union, the Limousin Regional Council, and the French National Institute for Agricultural Research. AP were supported by a PhD fellowship from INRA/Region Limousin and the Foundation for Medical Research.

DISCLOSURES

The authors have nothing to disclose.

AUTHOR CONTRIBUTIONS

A. Parenté, L. Magnol, and V. Blanquet designed research; A. Parenté, L. Magnol, and V. Blanquet analyzed data; A. Parenté, A. Boukredine, N. Duprat, F. Baraige performed experiments; A. Parenté and V. Blanquet wrote the paper.

REFERENCES

1. Pirruccello-Straub M, Jackson J, Wawersik S, et al. Blocking extracellular activation of myostatin as a strategy for treating muscle wasting. *Sci Rep*. 2018;8(1):2292.
2. Berchtold MW, Brinkmeier H, Müntener M. Calcium ion in skeletal muscle: its crucial role for muscle function, plasticity, and disease. *Physiol Rev*. 2000;80(3):1215-1265.
3. Chargé SBP, Rudnicki MA. Cellular and molecular regulation of muscle regeneration. *Physiol Rev*. 2004;84(1):209-238.
4. Ontell M, Kozeka K. The organogenesis of murine striated muscle: a cytoarchitectural study. *Am J Anat*. 1984;171(2):133-148.
5. White RB, Biérinx A-S, Gnocchi VF, Zammit PS. Dynamics of muscle fibre growth during postnatal mouse development. *BMC Dev Biol*. 2010;22(10):21.
6. Schiaffino S, Dyar KA, Ciciliot S, Blaauw B, Sandri M. Mechanisms regulating skeletal muscle growth and atrophy. *FEBS J*. 2013;280(17):4294-4314.
7. Sandri M. Signaling in muscle atrophy and hypertrophy. *Physiology*. 2008;23:160-170.
8. Lee S-J. Extracellular regulation of myostatin: a molecular rheostat for muscle mass. *Immunol Endocr Metab Agents Med Chem*. 2010;10:183-194.

9. McPherron AC, Lee SJ. Double muscling in cattle due to mutations in the myostatin gene. *Proc Natl Acad Sci USA*. 1997;94(23):12457-12461.
10. Dong J, Dong Y, Dong Y, Chen F, Mitch WE, Zhang L. Inhibition of myostatin in mice improves insulin sensitivity via irisin-mediated cross talk between muscle and adipose tissues. *Int J Obes*. 2016;40(3):434-442.
11. McPherron AC, Lee S-J. Suppression of body fat accumulation in myostatin-deficient mice. *J Clin Invest*. 2002;109(5):595-601.
12. Hoogaars WMH, Jaspers RT. Past, present, and future perspective of targeting myostatin and related signaling pathways to counteract muscle atrophy. *Adv Exp Med Biol*. 2018;1088:153-206.
13. Al-Zaidy SA, Sahenk Z, Rodino-Klapac LR, Kaspar B, Mendell JR. Follistatin gene therapy improves ambulation in becker muscular dystrophy. *J Neuromuscul Dis*. 2015;2(3):185-192.
14. Mendell JR, Sahenk Z, Al-Zaidy S, et al. Follistatin gene therapy for sporadic inclusion body myositis improves functional outcomes. *Mol Ther*. 2017;25(4):870-879.
15. Kondás K, Szláma G, Trexler M, Patthy L. Both WFIKKN1 and WFIKKN2 have high affinity for growth and differentiation factors 8 and 11. *J Biol Chem*. 2008;283(35):23677-23684.
16. Szláma G, Kondás K, Trexler M, Patthy L. WFIKKN1 and WFIKKN2 bind growth factors TGFβ1, BMP2 and BMP4 but do not inhibit their signalling activity. *FEBS J*. 2010;277(24):5040-5050.
17. Brun C, Monestier O, Legardinier S, Maftah A, Blanquet V. Murine GASP-1 N-glycosylation is not essential for its activity on C2C12 myogenic cells but alters its secretion. *Cell Physiol Biochem*. 2012;30(3):791-804.
18. Pèrié L, Parenté A, Brun C, Magnol L, Pélissier P, Blanquet V. Enhancement of C2C12 myoblast proliferation and differentiation by GASP-2, a myostatin inhibitor. *Biochem Biophys Rep*. 2016;3(6):39-46.
19. Monestier O, Brun C, Heu K, et al. Ubiquitous Gasp1 overexpression in mice leads mainly to a hypermuscular phenotype. *BMC Genom*. 2012;10(13):541.
20. Périè L, Parenté A, Baraige F, Magnol L, Blanquet V. Alterations in adiposity and glucose homeostasis in adult Gasp-1 overexpressing mice. *CPB*. 2017;44(5):1896-1911.
21. Brun C, Périé L, Baraige F, Vernus B, Bonnieu A, Blanquet V. Absence of hyperplasia in Gasp-1 overexpressing mice is dependent on myostatin up-regulation. *Cell Physiol Biochem*. 2014;34(4):1241-1259.
22. Grobet L, Pirottin D, Farnir F, et al. Modulating skeletal muscle mass by postnatal, muscle-specific inactivation of the myostatin gene. *Genesis*. 2003;35(4):227-238.
23. Meunier B, Picard B, Astruc T, Labas R. Development of image analysis tool for the classification of muscle fibre type using immunohistochemical staining. *Histochem Cell Biol*. 2010;134(3):307-317.
24. Oliver MH, Harrison NK, Bishop JE, Cole PJ, Laurent GJ. A rapid and convenient assay for counting cells cultured in microwell plates: application for assessment of growth factors. *J Cell Sci*. 1989;92(Pt 3):513-518.
25. Parenté A, Pèrié L, Magnol L, Bouhouche K, Blanquet V. A siRNA mediated screen during C2C12 myogenesis. *Methods Mol Biol*. 2019;1889:229-243.
26. Lee Y-S, Lee S-J. Regulation of GDF-11 and myostatin activity by GASP-1 and GASP-2. *Proc Natl Acad Sci USA*. 2013;110(39):E3713-E3722.
27. McPherron AC, Lawler AM, Lee SJ. Regulation of anterior/posterior patterning of the axial skeleton by growth/differentiation factor 11. *Nat Genet*. 1999;22(3):260-264.
28. Egerman M, Cadena S, Gilbert J, et al. GDF11 increases with age and inhibits skeletal muscle regeneration. *Cell Metab*. 2015;22(1):164-174.
29. Hammers DW, Merscham-Banda M, Hsiao JY, Engst S, Hartman JJ, Sweeney HL. Supraphysiological levels of GDF11 induce striated muscle atrophy. *EMBO Mol Med*. 2017;9(4):531-544.
30. Zhang Y, Wei Y, Liu D, et al. Role of growth differentiation factor 11 in development, physiology and disease. *Oncotarget*. 2017;8(46):81604-81616.
31. Walker RG, Angerman EB, Kattamuri C, Lee Y-S, Lee S-J, Thompson TB. Alternative binding modes identified for growth and differentiation factor-associated serum protein (GASP) family antagonism of myostatin. *J Biol Chem*. 2015;290(12):7506-7516.

How to cite this article: Parenté A, Boukredine A, Baraige F, et al. GASP-2 overexpressing mice exhibit a hypermuscular phenotype with contrasting molecular effects compared to GASP-1 transgenics. *The FASEB Journal*. 2020;00:1–15. https://doi.org/10.1096/fj.201901220R